Phase field simulation of grain size effects on the phase coexistence and magnetostrictive behavior near the ferromagnetic morphotropic phase boundary

Cite as: Appl. Phys. Lett. 115, 162402 (2019); https://doi.org/10.1063/1.5118927 Submitted: 06 July 2019 . Accepted: 27 September 2019 . Published Online: 14 October 2019

Cheng-Chao Hu $^{f f 0}$, Zhao Zhang, Tian-Nan Yang $^{f f 0}$, Yang-Guang Shi, Xiao-Xing Cheng $^{f f 0}$, Jun-Jie Ni, Ji-Gong Hao, Wei-Feng Rao, and Long-Qing Chen







View Online

ARTICLES YOU MAY BE INTERESTED IN

The structure and electronic properties of crimson phosphorus
Applied Physics Letters 115, 163101 (2019); https://doi.org/10.1063/1.5118860

Surface-induced thickness limit of conducting La-doped SrTiO₃ thin films Applied Physics Letters 115, 161601 (2019); https://doi.org/10.1063/1.5111771

Temperature-dependent spin Hall effect tunneling spectroscopy in platinum Applied Physics Letters 115, 162403 (2019); https://doi.org/10.1063/1.5121165

Lock-in Amplifiers up to 600 MHz







Phase field simulation of grain size effects on the phase coexistence and magnetostrictive behavior near the ferromagnetic morphotropic phase boundary

Cite as: Appl. Phys. Lett. **115**, 162402 (2019); doi: 10.1063/1.5118927 Submitted: 6 July 2019 · Accepted: 27 September 2019 · Published Online: 14 October 2019







Cheng-Chao Hu,^{1,2,a)} D Zhao Zhang,¹ Tian-Nan Yang,^{2,b)} D Yang-Guang Shi,³ Xiao-Xing Cheng,² D Jun-Jie Ni,¹ Ji-Gong Hao,¹ Wei-Feng Rao,^{4,c)} and Long-Qing Chen²

AFFILIATIONS

- ¹College of Materials Science and Engineering, Liaocheng University, Liaocheng 252059, China
- ²Department of Materials Science and Engineering, The Pennsylvania State University, University Park, Pennsylvania 16802, USA
- Department of Applied Physics, Nanjing University of Aeronautics and Astronautics, Nanjing 210016, China
- ⁴Department of Materials Processing, School of Mechanical and Automotive Engineering, Qilu University of Technology, Shandong Academy of Sciences, Jinan 250353, China
- a) Electronic mail: huchengchao@lcu.edu.cn
- b) Electronic mail: tuy123@psu.edu
- c)Electronic mail: wfrao@hotmail.com

ABSTRACT

The grain size effects on the phase coexistence and magnetostrictive response of $Tb_{1-x}Dy_xFe_2$ polycrystals near the ferromagnetic morphotropic phase boundary (MPB) are revealed through phase-field modeling. It shows that phase coexistence is a universal phenomenon in polycrystals for both ferromagnetic and ferroelectric MPB and that the range of compositions for phase coexistence increases with decreasing grain sizes. A large, reversible, and anhysteretic magnetostrictive response at low external fields is also found in the fine-grained polycrystals around the ferromagnetic MPB, which offers us a route to developing nanocrystalline magnetostrictive materials.

Published under license by AIP Publishing. https://doi.org/10.1063/1.5118927

Chemical and structural heterogeneities as well as the resulting interaction of two or more coexisting phases in functional oxides usually lead to extraordinary material properties, as observed in relaxor ferroelectrics and piezoelectric materials at the morphotropic phase boundary (MPB). 1-3 In the past few decades, many theoretical and experimental investigations have been devoted to seeking the origin of phase coexistence at the ferroelectric MPB and its effects on the material performance. 4-8 The concept of ferroelectric MPB was later physically parallelly extended to magnetostrictive alloy systems, i.e., the ferromagnetic MPB. 9-1 An excellent magnetoelastic response was also found near the ferromagnetic MPB. Recently, high resolution transmission electron microscopy has provided direct evidence for the coexistence of rhombohedral (R) and tetragonal (T) nanoscale domains (below 10 nm) in the giant magnetostrictive Tb_{0.3}Dy_{0.7}Fe₂ alloy. What is more, Zhou et al. have proposed another type of ferromagnetic

MPB system wherein a giant magnetic susceptibility with zero strain was found. ¹³ More recently, Ma *et al.* have revealed a sign-changed-magnetostriction effect of ferromagnetic MPB. ¹⁴ These studies show the increasing interest in ferromagnetic MPBs, which are a topic of both scientific and technological importance.

Our recent phase-field simulations on the temperature dependence of domain structures in the Tb_{0.27}Dy_{0.73}Fe₂ single crystal¹⁵ showed that phase coexistence with multidomain microstructures indeed appears in the vicinity of ferromagnetic MPB, which was consistent with the experimental results.¹² We further revealed the crucial role of long-range magnetostatic interaction and elastic interaction in the phase coexistence at the ferromagnetic MPB through energy analysis. The pictured kinetic path of domain evolution during field-induced phase transformations provides an opportunity to exploit the desired strain behaviors. However, in both experimental and theoretical works on the ferromagnetic MPB, most interest was paid to the

intrinsic contribution (in a single crystal), while little has been paid to the study of ferromagnetic MPB in polycrystals so far. In this paper, we report the grain size-dependent behavior of ferromagnetic MPB and the underlying mechanism of phase coexistence in ferromagnetic polycrystals through phase-field modeling. In particular, we propose a grain size effect on the magnetostrictive response of ferromagnetic polycrystals.

The grain structure and the domain structure in each individual grain are considered to describe the microstructure of a polycrystal. The total free energy of a ferromagnetic polycrystal system is written as 16

$$E_{tot} = \int_{V} (E_{ani} + E_{el} + E_{exc} + E_{ms} + E_{ext}) dV, \tag{1}$$

where E_{ani} denotes the magnetocrystalline anisotropy energy density, E_{el} the elastic energy density, E_{exc} the exchange energy density, E_{ms} the magnetostatic energy density, and E_{ext} the external field energy density. The domain structure within each grain is described by the inhomogeneous distribution of the local magnetization M_i^L , where i=1,2,3 and the superscript L indicates that the magnetization components are expressed in local coordinates within each individual grain. Therefore, the anisotropy energy density in a given grain can be given as 17

$$E_{ani} = K_1 \left[(m_1^L m_2^L)^2 + (m_2^L m_3^L)^2 + (m_3^L m_1^L)^2 \right] + K_2 (m_1^L m_2^L m_3^L)^2,$$
(2)

where K_1 and K_2 are the anisotropy constants and m_i^L are the components of the reduced magnetization vector, M_i^L/M_s . To solve the elasticity and magnetostatic equations, a common global coordinate system is introduced. Similar to the ferroelectric polycrystals, ¹⁸ the local magnetization M_i^L is related to the magnetization in the global system M_i through

$$M_i^L = R_{ij}M_j, (3)$$

where R_{ij} represents the grain rotation matrix field that describes the geometry (size, shape, and location) and crystallographic orientation of individual grains in the polycrystal. The elastic energy density is given in the global coordinate system by 19

$$E_{el} = \frac{1}{2} c_{ijkl} e_{ij} e_{kl} = \frac{1}{2} c_{ijkl} (\varepsilon_{ij} - \varepsilon_{ij}^0) (\varepsilon_{kl} - \varepsilon_{kl}^0), \tag{4}$$

where c_{ijkl} represents the elastic stiffness tensor, e_{ij} the elastic strain, ϵ_{ij} the total strain, and ϵ_{ij}^0 the spontaneous strain. In cubic magnetostrictive materials, the spontaneous strain denotes the spontaneous lattice deformation coupled to the local magnetization in a given grain and can be expressed by¹⁷

$$\varepsilon_{ij}^{0L} = \begin{cases} \frac{3}{2} \lambda_{100} \left(m_i^L m_j^L - \frac{1}{3} \right) & (i = j) \\ \frac{3}{2} \lambda_{111} m_i^L m_j^L & (i \neq j) \end{cases}$$
(5)

where λ_{100} and λ_{111} are the magnetostrictive constants. The spontaneous strain in the global coordinate system can be obtained from

$$\varepsilon_{ii}^0 = R_{ki} R_{li} \varepsilon_{kl}^{0L}. \tag{6}$$

According to the Khachaturyan theory on microelasticity,²⁰ the total strain ε_{ij} can be represented as the sum of the spatially

independent homogeneous strain $\bar{\epsilon}$ and a spatially dependent heterogeneous strain ϵ_{ij}^{het} , i.e.,

$$\varepsilon_{ij} = \bar{\varepsilon}_{ij} + \varepsilon_{ii}^{het}. \tag{7}$$

The homogenous strain determines the macroscopic shape deformation of the entire polycrystal resulting from an applied strain, phase transformations, or domain structure changes. If a constant strain ε^a_{ij} is applied to the entire system, $\bar{\varepsilon}_{ij} = \varepsilon^a_{ij}$; If the system is unconstrained and there is no stress applied, $\bar{\varepsilon}_{ij}$ is obtained by minimizing the total elastic energy with respect to the homogeneous strain. In this case, the homogenous strain is given by $\bar{\varepsilon}_{ij} = \bar{\varepsilon}^0_{ij}$, where $\bar{\varepsilon}^0_{ij}$ represents the intrinsic strain; If a constant stress σ^a_{kl} is applied, $\bar{\varepsilon}_{ij}$ is obtained by minimizing the sum of elastic energy and the potential of the mechanical loading with respect to the homogeneous strain. In this case, the homogeneous strain is given by 1^7

$$\bar{\varepsilon}_{ij} = s_{ijkl}\sigma^a_{kl} + \bar{\varepsilon}^0_{ii},\tag{8}$$

where s_{ijkl} are the three independent compliance constants for a cubic material in Voigt's notion. The equilibrium heterogeneous strain satisfies the mechanical equilibrium condition

$$\sigma_{ij,j} = 0, \tag{9}$$

where $\sigma_{ij,j}$ is the sum of the derivatives of elastic stress of σ_{ij} with respect to the j axis of global coordinates. For simplicity, we assume the elastic constants to be isotropic. The equilibrium heterogeneous strain can be solved using the Fourier transforms. The magnetic domain structures are obtained by numerically solving the kinetic (time-dependent Landau-Lifshitz-Gilbert) equation using the Gauss-Seidel projection method. The sum of the derivative of the sum of the control of the sum of the control of the sum of the sum of the control of the sum of the sum of the control of the sum of the

We performed quasi-two-dimensional numerical simulations to study the domain configuration and magnetostrictive response in ${\rm Tb_{1-x}Dy_xFe_2}$ polycrystals for computational reasons and simplicity although the model is applicable to three-dimensional polycrystalline systems. Polycrystalline structures with random grain orientations and different grain sizes are generated using the grain-growth model developed by Krill and Chen, ²² as shown in Fig. 1. Different polycrystalline

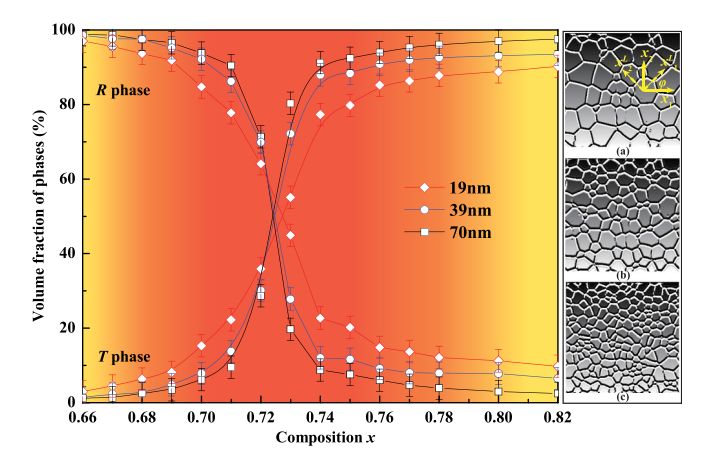


FIG. 1. Grain size-dependent phase coexistence phenomenon around ferromagnetic MPB in $Tb_{1-x}Dy_xFe_2$ polycrystals. (a)–(c) show the polycrystalline structures with different average grain sizes of 70, 39, and 19 nm, respectively.

structures with average grain sizes of 70, 39, and 19 nm were set as the inputs for the magnetic domain evolution. In the simulation, a system of $256\Delta \times 256 \Delta \times 4\Delta$ with a cell size of $\Delta=2$ nm was adopted, with the periodic boundary condition employed. The initial magnetic configuration was created by assigning random magnetization in each simulation cell. The corresponding material parameters were obtained from previous experimental and theoretical works. ^{16,23–26} Similar to the treatment by Bergstrom *et al.* ¹¹ and Atzmony *et al.* ²⁷ the anisotropy constants of Tb_{1-x}Dy_xFe₂ were set as $K_i(\text{Tb}_{1-x}\text{Dy}_x\text{Fe}_2) = (1-x)K_i(\text{TbFe}_2) + xK_i(\text{DyFe}_2)$, where K_i are the *i*th-order magnetocrystalline anisotropy constants. The composition range was chosen to vary within $0.66 \le x \le 0.82$. For each composition and grain size, the statistical average of 10 individual simulations with different random initial magnetization was applied to overcome the accidental error.

The average volume fraction of the tetragonal phase as a function of the composition x for different average grain sizes is illustrated in Fig. 1. It can be seen that the tetragonal phase fraction increases smoothly across the MPB from the Tb-rich (rhombohedral) side to the Tb-poor (tetragonal) side. That is, tetragonal and rhombohedral phases coexist over a composition range of $0.66 \le x \le 0.82$. This composition width of nanograins is much larger than that of micrograins.²⁸ As the grain size decreases, the number of tetragonal variants present in each grain decreases, and most of the grains become single domains when the average grain size decreases to 19 nm, as shown in Fig. 2(b). A similar grain size effect of phase distribution has also been observed in the experimental and theoretical works of ferroelectric polycrystals. 18,22,29 More importantly, the simulation also reveals a grain size effect of phase coexistence around the MPB of ferromagnetic polycrystals: The width of the phase coexistence composition range of $Tb_{1-x}Dy_xFe_2$ increases upon decreasing the grain size from 70 nm to 19 nm. The underlying mechanisms are revealed in Fig. 2.

Figure 2(a) shows the thermodynamic analysis of the anisotropy energy profile within the (110) plane for the compositions with x = 0.68, 0.72, 0.73, 0.75, and 0.80. As in the case of single crystals,

because of the low anisotropy energy barrier between rhombohedral $(M_s \parallel [111])$ and tetragonal $(M_s \parallel [100])$ phases in the vicinity of MPB, local energy minimum as well as the inhomogeneous internal stress distribution among the domain boundaries with multiple structure variants together give rise to a favorable bridging domain configuration and natural mechanism for phase coexistence. 15 Such a multidomain microstructure is also found in the polycrystal with the composition in the vicinity of MPB, especially for the larger nanograin system, as shown in Fig. 2(b). At both ends of the MPB, the energy barrier between the stable phase and the metastable phase becomes high, and it is difficult to overcome this barrier even if there might be additional energy arising from the lattice misfit and magnetization distribution among multiple domain variants (in/out of different grains). Thus, the volume fraction of the metastable phase decreases when the compositions deviated from the MPB. This mechanism gives rise to the composition-dependent phase coexistence behavior for the polycrystals with the same average grain size. On the other hand, it should be noted that the mechanical and magnetic configurations around the grain boundaries have significant effects on the phase-coexisting domain microstructures for the composition range around the ferromagnetic MPB. In polycrystals, high internal stresses usually develop around grain boundaries and especially their junctions as shown in Fig. 2(d), where magnetic charges also accumulate. As a result, minor domains of the metastable phase preferably form at grain boundaries and their junctions and then further extend toward the inside of grains. This grain boundary effect is more significant for ferromagnetic polycrystals with smaller grains. Taking x = 0.73 as an example, in Fig. 2(c), we can see that high anisotropy energy density mainly concentrates at the grain boundaries, and the average anisotropy energy density decreases upon decreasing the grain size from 70 nm to 19 nm. Moreover, the elastic energy density also concentrates around grain boundaries and especially their junctions, leading to an inhomogeneous magnetization distribution due to the magnetostrictive effect. As the grain size decreases from 70 nm to 19 nm, the total fraction of

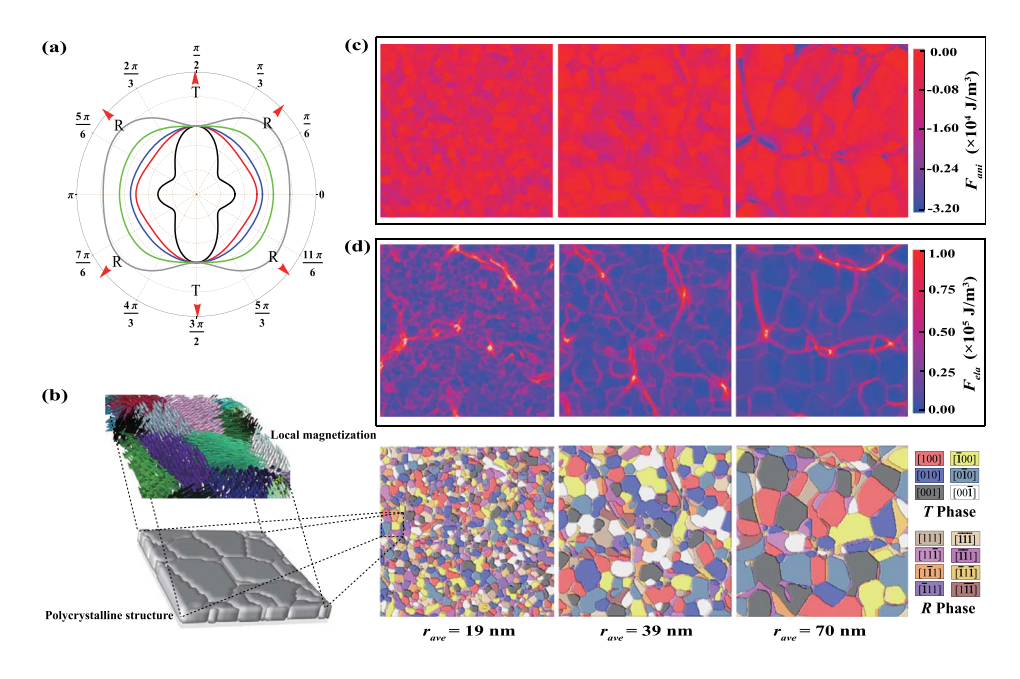


FIG. 2. (a) Thermodynamic analysis of the anisotropy energy profile within (110) for Tb_{0.27}Dy_{0.73}Fe₂ with different x values (the curves from inside to outside correspond to different x values of 0.68, 0.70, 0.72, 0.73, and 0.78). (b) Magnetization and domain structures of Tb_{0.27}Dy_{0.73}Fe₂ polycrystals with different average grain sizes of 70 nm, 39 nm, and 19 nm, respectively: T_1^+ : (1, 0, 0); T_1^- : (-1, 0, 0); T_2^+ : (0, 1, 0); T_2^- : (0, -1, 0); T_3^+ : (0, 0, 1); T_3^- : (0, 0, -1) R_1^+ : (1, 1, 1); and R_1^- : (-1, -1, -1); R_2^+ : (1, 1, -1); R_2^- : (-1, -1, 1); R_3^+ : (1, -1, 1); R_3^+ : (-1, 1, 1); R_4^- : (1, -1, -1). (c) Anisotropy and (d) elastic energy density distributions for the Tb_{0.27}Dy_{0.73}Fe₂ polycrystals with different average grain sizes of 70 nm, 39 nm, and 19 nm, respectively.

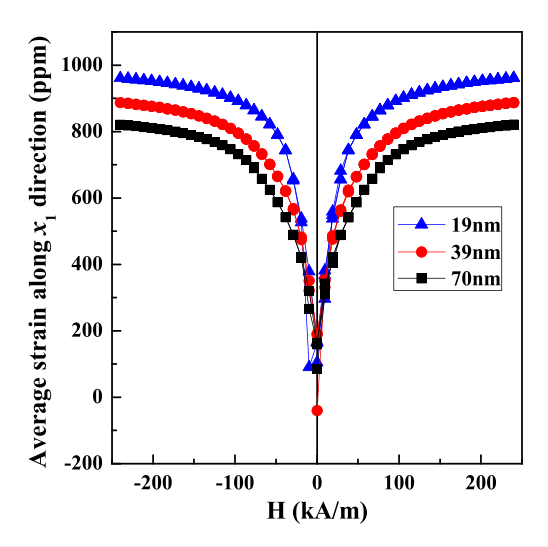


FIG. 3. Magnetostriction loops of $\mathsf{Tb}_{0.27}\mathsf{Dy}_{0.73}\mathsf{Fe}_2$ nanocrystals with grain sizes of 70, 39, and 19 nm.

grain boundaries in the polycrystal is gradually enriched, corresponding to the concentration of high internal stresses and the accumulation of magnetic charges. The lower anisotropy energy barrier, higher internal stresses, and corresponding magnetization distribution together give rise to the preferable formation of the metastable phase at the grain boundaries of smaller nanograins. This mechanism explains the size-dependent phase coexistence composition range for the polycrystals with different grain sizes.

In order to study the effect of the grain size on the magnetostrictive response, we constructed the strain-magnetic field loops of Tb_{0.27}Dy_{0.73}Fe₂ with different grain sizes of 70, 39, and 19 nm as presented in Fig. 3. A high-sensitive, low loss magnetostrictive behavior can be found in all nanocrystalline samples, and the average strain gradually increases with the decreasing grain size. As shown in Fig. 2, the grain boundaries are enriched with the decreasing grain size and most of the grains become single domains when the average grain size is 19 nm. The abundant grain boundaries act as sources for the nucleation of metastable phases, due to the large elastic energy concentrated around grain boundaries and their junctions. Similar to the ferroelectric MPB systems, fieldinduced stable-to-metastable phase transformation 30,31 gives rise to the increased domain reversibility and enhanced strain response. Therefore, the nanopolycrystal with a smaller grain size provides more nucleation sites for the phase transformation and domain switching, resulting in a large, reversible, and anhysteretic magnetostriction at low external fields. Grain refinement also supplies a method to further enhance the magnetoelastic response of magnetostrictive polycrystals, especially for the light-rare-earth-based RFe2 (R = rare earth) alloys which could not be readily transformed into single crystals or textured samples.

In conclusion, a grain size- and composition-dependent behavior of phase coexistence around the MPB in ferromagnetic polycrystals is revealed through phase-field modeling. It should be noted that a similar phenomenon was also proposed in ferroelectric MPB systems, which suggests a domain-level physical parallelism between ferromagnetic and ferroelectric MPBs. Furthermore, a large, reversible, and anhysteretic magnetostrictive response at low external fields is also found in the fine-grained polycrystals around the ferromagnetic MPB,

which will provide theoretical guidance for developing nanocrystalline magnetostrictive materials.

This work was supported by the National Science Foundation of China (Grant Nos. 51701091, 11475086, and 11474167). Tian-Nan Yang and Long-Qing Chen were supported by the National Science Foundation under Grant No. DMR-1744213. Xiao-Xing Cheng was supported by the U.S. Department of Energy, Office of Basic Energy Sciences, Division of Materials Sciences and Engineering under Award No. DE-FG02-07ER46417.

REFERENCES

¹B. Jaffe, W. R. Cook, and H. Jaffe, *Piezoelectric Ceramics* (Academic Press, New York, 1971).

²L. E. Cross, "Relaxor ferroelectrics," Ferroelectrics **76**, 241–267 (1987).

³K. Uchino, Ferroelectric Devices (Marcel Dekker, New York, 2000).

⁴S. E. Park and T. R. Shrout, J. Appl. Phys. **82**, 1804 (1997).

⁵M. Ahart, M. Somayazulu, R. E. Cohen, P. Ganesh, P. Dera, H. K. Mao, R. J. Hemley, Y. Ren, P. Liermann, and Z. G. Wu, Nature 451, 545 (2008).

⁶W. F. Liu and X. B. Ren, Phys. Rev. Lett. **103**, 257602 (2009).

⁷Y. U. Wang, J. Mater. Sci. 44, 5225–5234 (2009).

⁸F. Li, D. B. Lin, Z. B. Chen, Z. X. Cheng, J. L. Wang, C. C. Li, Z. Xu, Q. W. Huang, X. Z. Liao, L. Q. Chen, T. R. Shrout, and S. J. Zhang, Nat. Mater. 17, 349–354 (2018).
⁹R. E. Newnham, Acta Crystallogr., Sect. A 54, 729 (1998).

¹⁰S. Yang, H. Bao, C. Zhou, Y. Wang, X. Ren, Y. Matsushita, Y. Katsuya, M. Tanaka, K. Kobayashi, X. Song et al., Phys. Rev. Lett. 104, 197201 (2010).

¹¹R. Bergstrom, Jr., M. Wuttig, J. Cullen, P. Zavalij, R. Briber, C. Dennis, V. O. Garlea, and M. Laver, Phys. Rev. Lett. 111, 017203 (2013).

¹²T. Y. Ma, X. L. Liu, X. W. Pan, X. Li, Y. Z. Jiang, M. Yan, H. Y. Li, M. X. Fang, and X. B. Ren, Appl. Phys. Lett. **105**, 192407 (2014).

¹³C. Zhou, S. Ren, H. Bao, S. Yang, Y. Yao, Y. Ji, X. Ren, Y. Matsushita, Y. Katsuya, M. Tanaka *et al.*, Phys. Rev. B **89**, 100101(R) (2014).

¹⁴T. Y. Ma, X. L. Liu, J. M. Gou, Y. Wang, C. Wu, C. Zhou, Y. Wang, S. Yang, and X. B. Ren, Phys. Rev. Mater. 3, 034411 (2019).

¹⁵C. C. Hu, T. N. Yang, H. B. Huang, J. M. Hu, J. J. Wang, Y. G. Shi, D. N. Shi, and L. Q. Chen, Appl. Phys. Lett. **108**, 141908 (2016).

¹⁶ A. E. Clark, in *Ferromagnetic Materials*, edited by E. P. Wohlfarth (North-Holland, Amsterdam, 1980), Vol. 1, pp. 531.

¹⁷J. X. Zhang and L. Q. Chen, Acta Mater. **53**, 2845 (2005).

¹⁸S. Choudhury, Y. L. Li, C. E. Krill, and L. Q. Chen, Acta Mater. 55, 1415–1426 (2007).

¹⁹J. G. A. Rossetti, A. G. Khachaturyan, G. Akcay, and Y. Ni, J. Appl. Phys. 103, 114113 (2008).

²⁰A. G. Khachaturyan, Philos. Mag. **90**, 37 (2010).

²¹T. Mura, Micromechanics of Defects in Solids Distributors for the U.S. and Canada (Kluwer Academic Publishers, 1987).

²²C. E. Krill and L. Q. Chen, Acta Mater. **50**, 3059 (2002).

²³A. E. Clark, H. T. Savage, and M. L. Spano, IEEE Trans. Mag. **20**, 1443 (1984).

²⁴B. L. Wang and Y. M. Jin, J. Appl. Phys. **111**, 103908 (2012).

²⁵K. N. Martin, P. A. J. de Groot, B. D. Rainford, K. Wang, G. J. Bowden, J. P. Zimmermann, and H. Fangohr, J. Phys.: Condens. Matter 18, 459 (2006).

²⁶Y. C. Shu, M. P. Lin, and K. C. Wu, Mech. Mater. **36**, 975 (2004).

²⁷U. Atzmony, M. P. Dariel, E. R. Bauminger, D. Lebenbaum, I. Nowik, and S. Ofer, Phys. Rev. Lett. 28, 244 (1972).

²⁸ A. L. Janio, A. Branwood, R. Dudley, and A. R. Piercy, J. Phys. D: Appl. Phys. 20, 24–27 (1987).

²⁹W. F. Rao and Y. U. Wang, Appl. Phys. Lett. **92**, 102905 (2008).

³⁰L. Q. Chen, L. D. Chen, S. V. Kalinin, G. Klimeck, S. K. Kumar, J. Neugebauer, and I. Terasaki, npj Comput. Mater. 1, 15007 (2015).

³¹H. F. Li, npj Comput. Mater. **2**, 16032 (2016).

³²Y. G. Shi, C. C. Hu, J. Y. Fan, D. N. Shi, L. Y. Lv, and S. L. Tang, Appl. Phys. Lett. 101, 192405 (2012).

³³Z. Zhang, W. J. Lu, S. Z. Dong, H. R. Bai, T. N. Yang, D. H. Wei, J. J. Ni, W. Li, C. C. Hu, Y. G. Shi, H. Y. Li, J. G. Hao, P. Fu, and W. F. Rao, J. Magn. Magn. Mater. 471, 64–69 (2019).